AD-A066 130 ARMY ARMAMENT RESEARCH AND DEVELOPMENT COMMAND ABERD--ETC F/G 20/7
COMPUTER SIMULATION OF ELECTRON-BEAM-CAVITY INTERACTIONS IN COA--ETC(U)
JAN 79 R SHNIDMAN

UNCLASSIFIED ARBRL-TR-02131 SBIE-AD-E430 191 NL

| OF |
AD
A066130

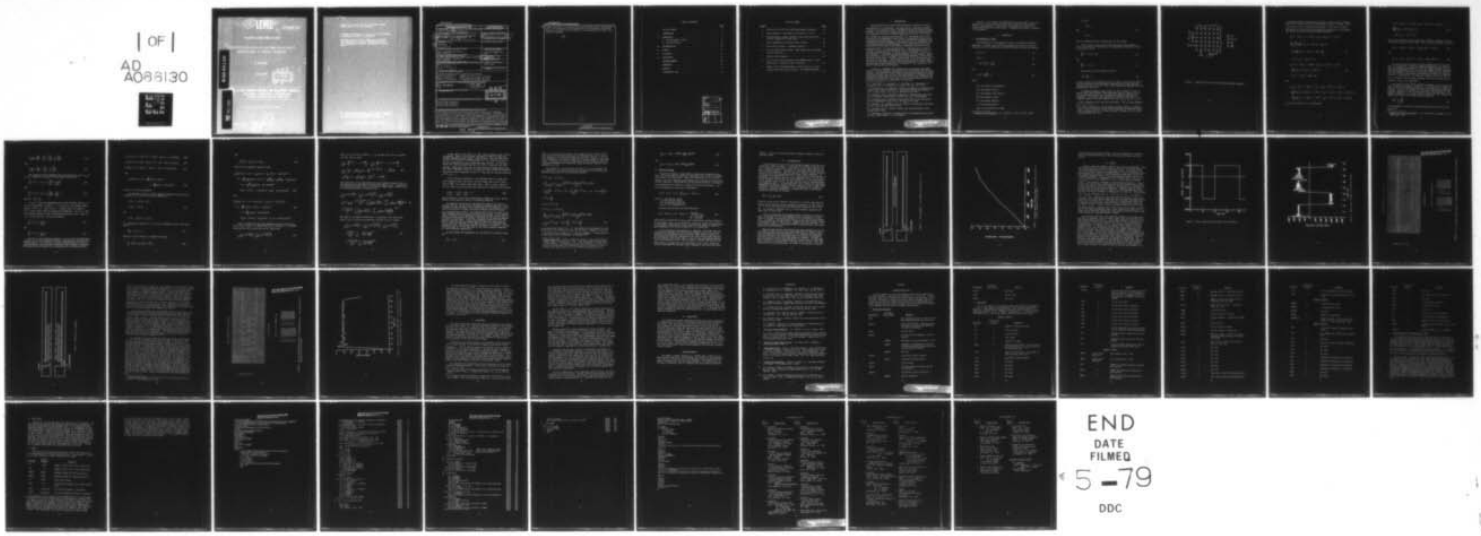

END
DATE
FILMED
5-79
DDC

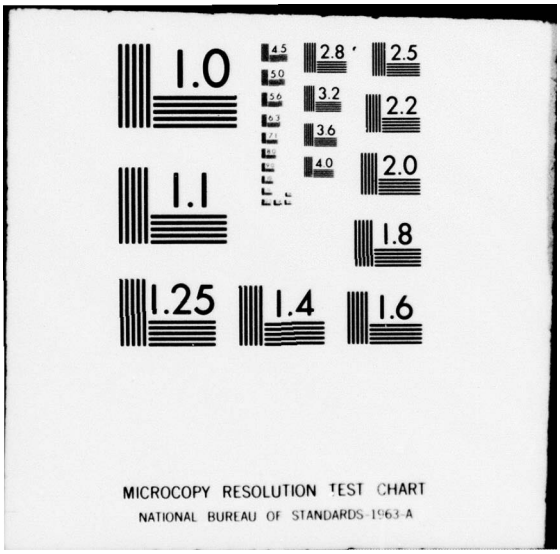
1.0
1.1
1.25
1.4
1.6
1.8
2.0
2.2
2.5
2.8
3.2
3.6
4.0
4.5
5.0
5.6
MICROCOPY RESOLUTION TEST CHART
NATIONAL BUREAU OF STANDARDS-1963-A

(12) LEVEL II

AD-E430 191

TECHNICAL REPORT ARBRL-TR-02131

COMPUTER SIMULATION OF ELECTRON-BEAM-CAVITY INTERACTIONS IN COAXIAL GEOMETRY

R. Shnidman

January 1979

US ARMY ARMAMENT RESEARCH AND DEVELOPMENT COMMAND
BALLISTIC RESEARCH LABORATORY
ABERDEEN PROVING GROUND, MARYLAND

Destroy this report when it is no longer needed.
Do not return it to the originator.

Secondary distribution of this report by originating or sponsoring activity is prohibited.

Additional copies of this report may be obtained from the National Technical Information Service, U.S. Department of Commerce, Springfield, Virginia 22161.

UNCLASSIFIED

SECURITY CLASSIFICATION OF THIS PAGE (When Data Entered)

REPORT DOCUMENTATION PAGE

READ INSTRUCTIONS BEFORE COMPLETING FORM

1. REPORT NUMBER (14) TECHNICAL REPORT ARBRL-TR-02131

2. GOVT ACCESSION NO.

3. RECIPIENT'S CATALOG NUMBER

4. TITLE (and Subtitle) (6) COMPUTER SIMULATION OF ELECTRON-BEAM-CAVITY INTERACTIONS IN COAXIAL GEOMETRY

5. TYPE OF REPORT & PERIOD COVERED (9) Technical rept.

6. PERFORMING ORG. REPORT NUMBER

7. AUTHOR(s) (10) R. Shnidman

8. CONTRACT OR GRANT NUMBER(s)

9. PERFORMING ORGANIZATION NAME AND ADDRESS
Ballistic Research Laboratory
ATTN: DRDAR-BLB
Aberdeen Proving Ground, MD 21005

10. PROGRAM ELEMENT, PROJECT, TASK AREA & WORK UNIT NUMBERS
61101A/1T161101A91A/00/
015AJ

11. CONTROLLING OFFICE NAME AND ADDRESS
US Army Armament Research & Development Command
Ballistic Research Laboratory
ATTN: DRDAR-BL
Aberdeen Proving Ground, MD 21005

12. REPORT DATE (11) JANUARY 1979

13. NUMBER OF PAGES
53

14. MONITORING AGENCY NAME & ADDRESS (if different from Controlling Office) (12) 50 pp

15. SECURITY CLASS. (of this report)
Unclassified

15a. DECLASSIFICATION/DOWNGRADING SCHEDULE

16. DISTRIBUTION STATEMENT (of this Report)

Approved for public release; distribution unlimited.

(18) SBIE (19) AD-E430 191

17. DISTRIBUTION STATEMENT (of the abstract entered in Block 20, if different from Report)

(16) 1T161101A91A (17) 00

DDC RECEIVED MAR 22 1979 B

18. SUPPLEMENTARY NOTES

19. KEY WORDS (Continue on reverse side if necessary and identify by block number)

Particle-beam accelerator
Particle-beam simulation
Particle-beam interaction

20. ABSTRACT (Continue on reverse side if necessary and identify by block number) (idk)

Computer simulation of electron beams interacting with electromagnetic pulses generated in internally switched cavities is presented. The formulation and properties of the algorithms for the electromagnetic field propagation and particle motion are given. Results are shown for coaxial geometry, first showing the electromagnetic pulse propagation properties in the absence of a beam and then the interaction with a beam. The calculated accelerated beam has a risetime of a fraction of a nanosecond and the quality of the accelerated beam (Continued)

DD FORM 1 JAN 73 1473 EDITION OF 1 NOV 65 IS OBSOLETE

UNCLASSIFIED

SECURITY CLASSIFICATION OF THIS PAGE (When Data Entered)

393 471

depends critically on the synchronization of the beam with the electromagnetic pulse. The limitations of the present version of the computer code and the directions for future work are discussed. A users guide for the code is provided as an appendix.

TABLE OF CONTENTS

		Page
	LIST OF FIGURES	5
I.	INTRODUCTION	7
II.	FORMULATION	8
	A. Electromagnetic Fields	8
	B. Particle Pushing	19
III.	IMPLEMENTATION	20
IV.	RESULTS	23
V.	DISCUSSION	31
VI.	CONCLUSIONS	33
	ACKNOWLEDGEMENTS	33
	REFERENCES	35
	APPENDIX	37
	DISTRIBUTION LIST	51

LIST OF FIGURES

Figure		Page
1	Space grid for the finite difference Maxwell equation . . .	10
2	Cavity geometry: the length of the cavity is 1.8 m	21
3	Percent numeric voltage overshoot versus time step for an initial risetime of 15 time steps	22
4	Ideal transmission line open circuit voltage	24
5	Open circuit voltage - simulation results	25
6	B_θ 4 ns after switch closing. Every other point is plotted in the Z direction	26
7	Baffled cavity geometry	27
8	B_θ 6 ns after switch closing in the baffled cavity. Every other point is plotted in the Z direction	29
9	Energy of the accelerated beam in units of $m_c c^2$ as a function of time after switch closing. The injected beam has $\gamma = 2$	30

I. INTRODUCTION

High-current pulsed electron beam accelerator concepts are being investigated in our laboratory. One particularly interesting concept[1] is based on accelerating sections containing charged internally-switched elements. By closing the various switches in the proper synchronization, electromagnetic pulses are produced that would accelerate pulsed beams. This concept has recently been analyzed[2,3] by considering the cavities in which the electromagnetic pulses travel as transmission lines and applying principal mode theory. It was soon realized that geometries that correspond to constant-impedance transmission lines are advantageous for producing uniformly accelerated beams. Pulse distortions at the line discontinuities are being investigated by employing equivalent circuit representation[2,4-7] of the discontinuities. Although such an analysis provides a closed form representation to the time dependence of the resulting accelerating pulse, it leaves much to be desired. Firstly, as the frequency is increased the lumped parameters become frequency dependent and above a critical frequency the entire equivalent circuit representation breaks down. Secondly, complications arise when discontinuities are close to each other. And thirdly the value of the equivalent parameters is not available for many interesting geometries. Another feature not addressed by the transmission line analysis is the coupling of the beam to the accelerating structure.

In order to complement the transmission line analysis and address the above issues, computer simulations with electron beams have been performed. A two-dimensional axi-symmetric code was obtained from the Naval Research Laboratory that directly integrates Maxwell's equations and then accelerates charged particles with the resulting fields. Additions and modifications were made to the code so that it would address some of the questions raised by the transmission-line analysis.

---

[1] *A.I. Pavlovskii, V.S. Bosamykin, G.D. Kuleshev, A.I. Gerasimov, V.A. Tannankin, and A.P. Klementev, Sov. Phys. Dokl. 20, 441, (1975).*

[2] *D. Eccleshall and J.K. Temperley, "Transfer of Energy from Charged Transmission Lines With Applications to Pulsed High-Current Accelerators," Jour. of Appl. Phys., Vol. 49, pp. 3649-3655, July 1978.*

[3] *J.K. Temperley and D. Eccleshall, "Analysis of Transmission-Line Accelerator Concepts," ARBRL Report TR-02067, May 1978.* (AD #A0563634)

[4] *J.R. Whinnery and H.W. Jamieson, "Equivalent Circuits for Discontinuities in Transmission Lines," Proc. IRE 32, 98-115, 1944.*

[5] *J.R. Whinnery, H.W. Jamieson, and T.E. Robbins, "Coaxial-Line Discontinuities," Proc. IRE 32, 695-709, 1944.*

[6] *J.R. Whinnery and D.C. Stinson, "Radial Line Discontinuities," Proc. IRE 43, 46-51, 1955.*

[7] *J.K. Temperley, "Analysis of Coupling Region in Transmission-Line Accelerators," ARBRL Report (to be published).*

Section II will present the formulation and limitations of the code, and Section III will describe how the code is applied to the current problem. The remainder of this report is devoted to the results, discussion and direction for future work. A program users guide is provided in the Appendix.

II. FORMULATION

A. Electromagnetic Fields

The propagation of electromagnetic fields is governed by Maxwell's equations. In their usual form[8] the equations are written as (we use Gaussian units since these are the units for which the code was written)

$$\nabla \cdot \vec{D} = 4\pi\rho \quad , \tag{1}$$

$$\nabla \cdot \vec{B} = 0 \quad , \tag{2}$$

$$\nabla \times \vec{H} = \frac{4\pi}{c} \vec{J} + \frac{1}{c} \frac{\partial \vec{D}}{\partial t} \quad , \tag{3}$$

and

$$\nabla \times \vec{E} + \frac{1}{c} \frac{\partial \vec{B}}{\partial t} = 0 \quad , \tag{4}$$

where

$\vec{D}$ is the electric displacement,

$\vec{E}$ is the electric field,

$\vec{B}$ is the magnetic flux density,

$\vec{H}$ is the magnetic field,

$\vec{J}$ is the current density,

ρ is the charge density,

and c is the velocity of light.

---

[8] *Classical Electrodynamics*, J.D. Jackson, p. 178, J. Wiley, 1962.

In vacuo

$$\vec{D} = \vec{E}$$

and (5)

$$\vec{B} = \vec{H} .$$

We will consider only the in vacuo case for this report.

If the initial values of the fields are given and knowledge of their time evolution is desired, it is convenient to write eqs. (3 and 4) using eqs. (5) as

$$\frac{\partial \vec{E}}{\partial t} = c \nabla \times \vec{B} - 4\pi \vec{J} \tag{6}$$

and

$$\frac{\partial \vec{B}}{\partial t} = - c \nabla \times \vec{E}. \tag{7}$$

Application of the continuity equation

$$\nabla \cdot \vec{J} + \frac{\partial \rho}{\partial t} = 0 \tag{8}$$

to eqs. (6 and 7) will show that if eqs. (1 and 2) are initially obeyed they will continue to be obeyed when subjected to the time evolution prescribed by eqs. (6 and 7); thus a time integration algorithm need only consider eqs. (6 and 7).

A staggered-leapfrog scheme similar to that of Boris[9] is used to advance the E and B fields. The space grids used are shown in Fig. 1. For our present purposes only the transverse magnetic (TM) modes are considered. This restriction combined with the two-dimensional axi-symmetric nature of the code implies that only the E_Z, E_R, B_θ, J_R, and J_Z field components enter into the calculations. The J_R field component

[9] *J.P. Boris, "Relativistic Plasma Simulation-Optimization of a Hybrid Code," in the Proceedings of the Fourth Conference on Numerical Simulation of Plasmas, Ed. by J.P. Boris and Rama C. Shanny, pp. 3-67, Naval Research Laboratory, 1970.*

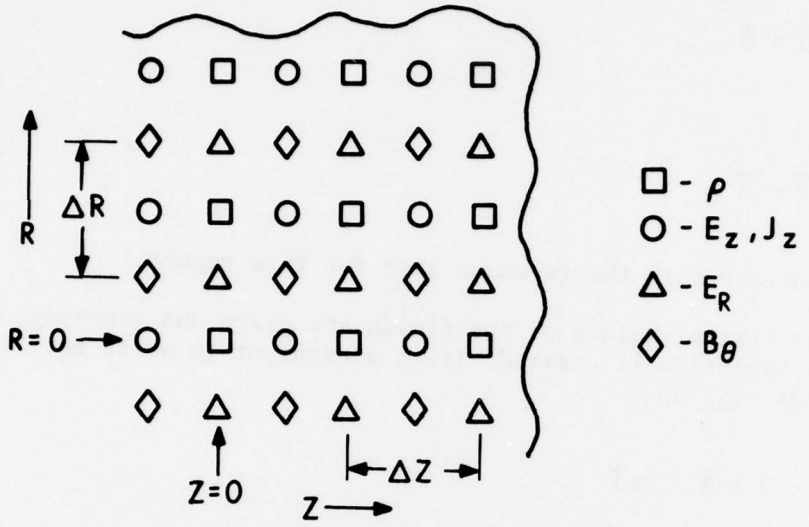

Figure 1. Space grid for the finite difference Maxwell equations

is suppressed because allowing the particles a radial degree of freedom would lead to beam blow-up if no stabilizing B_Z field is present. Such a B_Z field of course introduces non-TM modes. Later we will justify and explain the motivation for limiting the calculations to the TM modes. The fields are evolved with the following equations:

$$E_Z\ (Z - \Delta Z/2,\ R,\ T + \Delta T/2) = E_Z(Z - \Delta Z/2,\ R,\ T - \Delta T/2) +$$

$$\frac{c\Delta T}{\Delta R}\left[\frac{2R + \Delta R}{2R}\ B_\theta\ (Z - \Delta Z/2,\ R + \Delta R/2,\ T)\right.$$

$$\left. - \frac{2R - \Delta R}{2R}\ B_\theta\ (Z - \Delta Z/2,\ R - \Delta R/2,\ T)\right] \qquad (9)$$

$$- 4\pi\ \Delta T\ J_Z\ (Z - \Delta Z/2,\ R,\ T)\ ,$$

$$E_R\ (Z,\ R - \Delta R/2,\ T + \Delta T/2) = E_R\ (Z,\ R - \Delta R/2,\ T - \Delta T/2)$$

$$- \frac{c\Delta T}{\Delta Z}\ [B_\theta\ (Z + \Delta Z/2,\ R - \Delta R/2,\ T) \qquad (10)$$

$$- B_\theta\ (Z - \Delta Z/2,\ R - \Delta R/2,\ T)],$$

and

$$B_\theta\ (Z - \Delta Z/2,\ R - \Delta R/2,\ T + \Delta T) = B_\theta\ (Z - \Delta Z/2,\ R - \Delta R/2,\ T)$$

$$+ \frac{c\Delta T}{\Delta R}\ [E_Z\ (Z - \Delta Z/2,\ R,\ T + \Delta T/2) - E_Z\ (Z - \Delta Z/2,\ R - \Delta R,\ T + \Delta T/2)] \qquad (11)$$

$$- \frac{c\Delta T}{\Delta Z}\ [E_R\ (Z,\ R - \Delta R/2,\ T + \Delta T/2) - E_R\ (Z - \Delta Z,\ R - \Delta R/2,\ T + \Delta T/2)]\ .$$

On the axis (R=0) eq. (9) is replaced by

$$E_Z\ (Z - \Delta Z/2,\ 0,\ T + \Delta/2) = E_Z\ (Z - \Delta Z/2,\ 0,\ T - \Delta T/2) +$$

$$\frac{4c\Delta T}{\Delta R}\ B_\theta\ (Z - \Delta Z/2,\ \Delta R/2,\ T) \qquad (12)$$

$$- 4\pi\Delta T\ J_Z\ (Z - Z/2,\ 0,\ T)\ .$$

This equation follows from an application of Stokes' theorem. Also on the axis B_θ and E_R are set to zero. This is done in practice by setting

$$E_R\ (Z,\ -\Delta R/2,\ T + \Delta T/2) = -\ E_R(Z,\ \Delta R/2,\ T + \Delta T/2) \qquad (13)$$

and

$$B_\theta\ (Z - \Delta Z/2,\ -\Delta R/2,\ T) = -\ B_\theta\ (Z - \Delta Z/2,\ \Delta R/2,\ T)\ . \qquad (14)$$

The code at present allows only those boundaries which lie along the Z or R directions. Perfectly conducting boundaries are assumed; thus the tangential components of E and the normal component of B are zero on the boundaries. With our restricted number of field components, only the boundary conditions on E enter into consideration. The code sets the E field to zero within the conductors by means of rectangular (in an R, Z plane) masks. Two masks are required, one for E_R and one for E_Z, because of the different boundary conditions and grid point locations of these field components.

The solution of the finite difference equations (9-14) are not the exact solutions to Maxwell's equations. An effective way to judge how good are the finite difference solutions is to examine their dispersion relation. First we will examine the dispersion relations for the differential equations so that we will have a basis for comparison. From Maxwell's equation it is a simple matter to show that, in a charge free region, the electric field obeys the wave equation,

$$\nabla^2\vec{E} = \frac{1}{c^2}\frac{\partial^2\vec{E}}{\partial t^2}\ . \qquad (15)$$

For our geometry we obtain the following equations for the field components;[10]

---

[10] Methods of Theoretical Physics, P.M. Morse and H. Feshbach, p. 116, McGraw-Hill, 1953.

$$\frac{1}{R}\frac{\partial}{\partial R}\left(R\frac{\partial E_R}{\partial R}\right) - \frac{E_R}{R^2} + \frac{\partial^2 E_R}{\partial Z^2} = \frac{1}{c^2}\frac{\partial^2 E_R}{\partial t^2} \tag{16}$$

and

$$\frac{1}{R}\frac{\partial}{\partial R}\left(R\frac{\partial E_Z}{\partial R}\right) + \frac{\partial^2 E_Z}{\partial Z^2} = \frac{1}{c^2}\frac{\partial^2 E_Z}{\partial t^2} \quad . \tag{17}$$

Now assume the field components have the form $R^n \exp [i(\omega t + k_R R + k_Z Z)]$. Equations (16) and (17) then become respectively:

$$\frac{\omega^2}{k^2} = c^2 \left[1 - (2n + 1)\frac{ik_R}{k^2 R} + \frac{1 - n^2}{k^2 R^2}\right] \tag{18}$$

and

$$\frac{\omega^2}{k^2} = c^2 \left[1 - (2n + 1)\frac{ik_R}{k^2 R^2} - \frac{n^2}{k^2 R^2}\right] , \tag{19}$$

where $k^2 = k_R^2 + k_Z^2$.

If $k_R = 0$, then any propagating part of the field must have $E_Z = 0$; and it is convenient to choose $n = -1$ so that eq. (18) becomes nondispersive, $\omega^2/k^2 = c^2$. (The choice $n = 1$ would violate the equation $\nabla \cdot \vec{E} = 0$ that results from our charge-free assumption.) If $k_R \neq 0$, then for stability reasons to keep the dispersion relations real, n must be $-\frac{1}{2}$. In this case eqs. (18) and (19) become

$$\frac{\omega^2}{k^2} = c^2 \left(1 + \frac{3}{4k^2 R^2}\right) \tag{20}$$

and

$$\frac{\omega^2}{k^2} = c^2 \left(I - \frac{1}{4k^2 R^2}\right) \quad . \tag{21}$$

Now back to the difference equations. Just as with the differential equations, it is most convenient to derive the dispersion relations from a wave equation. We now derive the finite difference form of the wave equation directly from the finite difference form of Maxwell's equations. The notation may be simplified by introducing the following operators:

$$\partial_T X(Z, R, T) \equiv [X(Z, R, T + \Delta T/2) - X(Z, R, T - \Delta T/2)]/\Delta T, \quad (22)$$

$$\partial_Z X(R, Z, T) \equiv [X(Z + \Delta Z/2, R, T) - X(Z - \Delta Z/2, R, T)]/\Delta Z, \quad (23)$$

$$\partial_R X(R, Z, T) \equiv [X(Z, R + \Delta R/2, T) - X(Z, R - \Delta R/2, T)]/\Delta R, \quad (24)$$

and

$$\partial'_R X(R,Z,T) \equiv [(1 + \frac{\Delta R}{2R})X(Z,R + \Delta R/2,T) - (1 - \frac{\Delta R}{2R})X(Z,R - \Delta R/2,T)]/\Delta R, \quad (25)$$

where X is any field component.

We note that all pairs of these operators commute except ∂_R and ∂'_R. Equations (9-11) can now be written compactly as

$$\partial_T E_Z = c\,\partial'_R B_\theta - 4\pi J_Z,$$

$$\partial_T E_R = -c\partial_Z B_\theta \quad , \quad (26)$$

and

$$\partial_T B_\theta = c[\partial_R E_Z - \partial_Z E_R] \quad .$$

In a charge-free region $\nabla \cdot \vec{E} = 0$; the finite difference form of this equation is

$$\partial'_R E_R + \partial_Z E_Z = 0 \quad . \quad (27)$$

From eqs. (26,27) follow in a charge-free region

$$\frac{1}{c^2}\,\partial_T^2 E_R = \partial_R \partial'_R E_R + \partial_Z^2 E_R \quad (28)$$

and

$$\frac{1}{c^2}\,\partial_T^2\,E_Z = \partial_R\,\partial_E\,E_Z + \partial_Z^2\,E_Z \quad . \tag{29}$$

These last two equations expand to read

$$\frac{1}{c^2}\,[E_R(Z,R,T+\Delta T) - 2\,E_R(Z,R,T) + E_R\,(Z,R,\,T-\Delta T)]/(\Delta T)^2 =$$

$$[(1+\frac{\Delta R}{2R+\Delta R})E_R(Z,R+\Delta R,\,T) + (\frac{\Delta R}{2R+\Delta R} - \frac{\Delta R}{2R-\Delta R} - 2)E_R(Z,R,T)$$

$$+ (1 - \frac{\Delta R}{2R-\Delta R})E_R(Z,R-\Delta R,\,T)]/(\Delta R)^2 \;+$$

$$[E_R(Z+\Delta Z,R,T) - 2\,E_R(Z,R,T) + E_R(Z-\Delta Z,R,T)]/(\Delta Z)^2 \tag{30}$$

and

$$\frac{1}{c^2}\,[E_Z(Z,\,R,T+\Delta T) - 2E_Z(Z,R,T) + E_Z(Z,R,T-\Delta T)]/(\Delta T)^2 =$$

$$[(1+\frac{\Delta R}{2R})\,E_Z(Z,R+\Delta R,T) - 2\,E_Z(Z,R,T) \tag{31}$$

$$+ (1 - \frac{\Delta R}{2R})\,E_Z(Z,R-\Delta R,T)]/(\Delta R)^2$$

$$+(E_Z(Z+\Delta Z,R,T) - 2\,E_Z(Z,R,T) + E_Z\,(Z-\Delta Z,R,T)]/(\Delta Z)^2 \quad .$$

Again we assume that the field components have the form $R^n \exp [i(\omega t + k_R R + k_Z Z)]$. As before when $k_R = 0$, we take $n = -1$; and the resulting form for E_R inserted into eq. (30) yields

$$\frac{1}{(c\Delta T)^2}\sin^2\left(\frac{\omega\Delta T}{2}\right) = \frac{1}{(\Delta Z)^2}\sin^2\left(\frac{k_Z\,\Delta Z}{2}\right) . \tag{32}$$

When $k_R \neq 0$, we take as before $n = -\frac{1}{2}$; and when this form is inserted into eq. (30) we obtain

$$\frac{1}{(c\Delta T)^2}\left(e^{i\omega\Delta T} - 2 + e^{-i\omega\Delta T}\right) = \frac{1}{(\Delta Z)^2}\left(e^{ik_Z \Delta Z} - 2 + e^{-ik_Z \Delta Z}\right)$$

$$+ \frac{1}{(\Delta R)^2}\left[\left(1 + \frac{\Delta R}{2R + \Delta R}\right)\left(1 + \frac{\Delta R}{R}\right)^{-1/2} e^{ik_R \Delta R} - 2 + \frac{\Delta R}{2R + \Delta R}\right. \qquad (33)$$

$$\left. - \frac{\Delta R}{2R - \Delta R} + \left(1 - \frac{\Delta R}{2R - \Delta R}\right)\left(1 - \frac{\Delta R}{R}\right)^{-1/2} e^{-ik_R \Delta R}\right] .$$

The coefficient of the exponentials are then expanded in power series of $\Delta R/R$ and the resulting series are multiplied term by term. Proceeding in a straightforward manner after collecting the common powers of $\Delta R/R$ yields the following dispersion relation for E_R

$$\frac{1}{(c\Delta T)^2}\sin^2\left(\frac{\omega\Delta T}{2}\right) = \frac{1}{(\Delta R)^2}\sin^2\left(\frac{k_R \Delta R}{2}\right) + \frac{1}{(\Delta Z)^2}\sin^2\left(\frac{k_Z Z}{2}\right)$$

$$+ \frac{1}{8R^2 - 2(\Delta R)^2} - \frac{\cos(k_R \Delta R)}{2R^2}\sum_{n=0}^{\infty}\left\{\frac{1}{2^{4n+4}}\binom{4n+4}{2n+2} - \sum_{m=0}^{2n+1}\frac{1}{2^{2n+m+2}}\binom{2m}{m}\right\}\frac{\Delta R}{R}^{2n} \qquad (34)$$

$$+ \frac{i\sin(k_R \Delta R)}{2R^2}\sum_{n=1}^{\infty}\left\{\frac{1}{2^{4n+2}}\binom{4n+2}{2n+1} - \sum_{m=0}^{2n}\frac{1}{2^{2n+m+1}}\binom{2m}{m}\right\}\left(\frac{\Delta R}{R}\right)^{2n-1} ,$$

where $\binom{a}{b}$ is the binomial coefficient. Proceeding in the same manner from eq. (31) we obtain the dispersion relation for E_Z as follows,

$$\frac{1}{(c\Delta T)^2}\sin^2\left(\frac{\omega\Delta T}{2}\right) = \frac{1}{(\Delta R)^2}\sin^2\left(\frac{k_R \Delta R}{2}\right) + \frac{1}{(\Delta Z)^2}\sin^2\left(\frac{k_Z Z}{2}\right)$$

$$- \frac{\cos(k_R R)}{16R^2}\sum_{n=0}^{\infty}\binom{4n+2}{2n}\left(\frac{\Delta R}{4R}\right)^{2n} \qquad (35)$$

$$+ \frac{i\sin(k_R \Delta R)}{16R^2}\sum_{n=0}^{\infty}\binom{4n+4}{2n+1}\left(\frac{\Delta R}{4R}\right)^{2n+1} .$$

In the limit ΔT, ΔR, and $\Delta Z \to 0$, eqs. (34-35) reduce to eqs. (20-21) as expected. Now if we do not want the numeric solution to have non-physical exponential time growth, ω must be real. The last term in eqs. (34-35) will contribute an imaginary part to ω if k_R and k_Z are real, but this contribution is only significant near the axis. As the pulse leaves this region (remember now $k_R \neq 0$), $\Delta R/R \to 0$ and this last term vanishes. What these terms mean is that we have not chosen exactly correct radial dependences near the axis for the finite difference equations. The correct radial dependence is not $R^{-1/2}$ near the axis but does approach $R^{-1/2}$ as $R \to \infty$.

A most serious contribution to the imaginary part of ω would come from having the right side of eqs. (34-35) larger than $1/(c\,\Delta T)^2$ since then $\sin \frac{\omega \Delta T}{2}$ will become larger than unity. Thus to insure stability for all values of k_R and k_Z the time steps must be limited by the relation

$$\frac{1}{(c\,\Delta T)^2} > \frac{1}{(\Delta R)^2} + \frac{1}{(\Delta T)^2} + Q \quad , \tag{36}$$

where Q consists of the terms containing the summations in eqs. (34-35). Usually we may neglect Q since it is generally negative.

An important consequence of the difference between the exact dispersion relations and the finite difference dispersion relations is that although the lower frequency finite difference wave propagates at essentially the velocity of light, the higher frequency finite difference waves propagate more slowly.[9] Thus square pulses would have their rise-times degraded and would develop overshoots and ringing. These annoying numeric artifacts may be minimized by smoothing out the rise and fall of an injected square pulse and taking a fine mesh if the required computer resources are available. It has been determined empirically that the numeric overshoots reach a maximum amplitude above the square pulse of $(4/\pi - 1)$ times the amplitude of the square pulse if no reflections from boundaries occur. Reflections increase the amount of overshoot. We note in passing that $4/\pi$ is the amplitude of the lowest frequency component of a unit amplitude square pulse.

We now consider the formulation for the solution of Poisson's equation

$$\nabla^2 \phi = -4\pi\rho \quad , \tag{37}$$

where ϕ is the electric potential. This equation arises when we would like to know the potential and electric field components due to the initial charging up of electrodes within the cavities. Usually $\rho = 0$; however, the general case can be handled with a minimum amount of additional effort. Reference 11 contains a good discussion of relaxation and overrelaxation techniques for solving the finite difference equation corresponding to eq. (37).

The potential is specified on all points of a closed boundary and the potential at the interior points for our geometry are obtained from successive application of the following formulae

$$\phi^{(n+1)}(Z,R) = \phi^{(n)}(Z,R) +$$

$$+ \beta \left\{ \frac{1}{2/(\Delta Z)^2 + 2/(\Delta R)^2} \left[\frac{\phi^{(n)}(Z + \Delta Z,R) + \phi^{(n)}(Z - \Delta Z,R)}{(\Delta Z)^2} \right.\right.$$

$$\left.\left. + \frac{R + \Delta R/2}{R(\Delta R)^2} \phi^{(n)}(Z,R + \Delta R) + \frac{R - \Delta R/2}{R(\Delta R)^2} \phi^{(n)}(Z,R - \Delta R) - 4\pi\rho(Z,R) \right] \right.$$

$$\left. - \phi^{(n)}(Z,R) \right\} . \qquad (38)$$

On the axis we use

$$\phi^{(n+1)}(Z,0) = \phi^{(n)}(Z,0) +$$

$$+ \beta \left\{ \frac{1}{2/(\Delta Z)^2 + 4/(\Delta R)^2} \left[\frac{\phi^{(n)}(Z + \Delta Z,0) + \phi^{(n)}(Z - \Delta Z,0)}{(\Delta Z)^2} \right.\right.$$

$$\left.\left. + \frac{4}{(\Delta R)^2} \phi^{(n)}(Z,\Delta R) - 4\pi\rho(Z,0) \right] - \phi^{(n)}(Z,0) \right\} . \qquad (39)$$

An overrelaxation factor of $\beta = 1.7$ was found to be satisfactory for our application. We iterated with eqs. (38-39) until ϕ changed by less than a specified factor of usually 10^{-7} times the maximum ϕ. Having obtained ϕ, the electric field components are computed from

---

[11] *Space-Charge Flow*, Peter T. Kirstein, George S. Kino, and William E. Walters, Chap. 9, McGraw-Hill, 1967. Some typographical errors exist in this chapter. Of interest to us are the following: the factor h^2 should be removed from the denominator before the brackets in eq. (3.1) and the last terms of eqs. (3.2, 3.4) should be multiplied by h^2.

$$E_R(Z,R - \Delta R/2) = \frac{\phi(Z,R - \Delta R) - \phi(Z,R)}{\Delta R} \tag{40}$$

and

$$E_Z(Z - \Delta Z/2,R) = \frac{\phi(Z - \Delta Z,R) - \phi(Z,R)}{\Delta Z} . \tag{41}$$

B. Particle Pushing

The particle motion is prescribed by relativistic equations of motion. All of the particle motion is constrained to be in the Z direction for reasons to be given later. Under this constraint the E_Z field component is the only computed field component that provides an acceleration in the Z direction. The value of E_Z at a particle position is calculated by interpolating the values of E_Z from the 4 nearest mesh points. The particle momentum per unit mass is advanced by

$$P(T,I) = P(T - \Delta T,I) + \frac{Q}{M} E_{INT} (T - \Delta T/2) \Delta T \tag{42}$$

where I is the particle index,
Q is the particle charge,
M is the particle mass, and
E_{INT} is the interpolated E_Z.

The particle positions are then advanced by

$$Z(T + \Delta T/2,I) = Z(T - \Delta T/2,I) + \frac{P(T,I)\Delta T}{\sqrt{1 + \left[\frac{P(T,I)}{C}\right]^2}} . \tag{43}$$

Each particle contributes to the J_Z and ρ fields by an inverse interpolation procedure; that is, the particle's charge and current are apportioned to the nearest corresponding 4 grid points with the amount of apportionment depending on how close the particle is to a grid line.

A soft injection of the particles is employed. This means that the particles are "created" with their initial energy one-half of grid spacing before the beginning of the field grids. Until these so-called inactive particles reach the beginning of the field lattice these particles do not respond to the fields--that is, they are not accelerated; however they still contribute to the ρ and J_Z fields. Likewise upon leaving the field lattice, the particle still contribute to the ρ and J fields but are not accelerated for one half lattice spacing at the end of the field

lattice. We will say more about these transition regions in the discussion section.

III. IMPLEMENTATION

A cross-sectional view of the cylindrically-symmetric cavity to be simulated is shown in Figure 2. Initially the cylinder within the cavity is placed at a specified voltage and all of the other surfaces are held at ground potential. The switch is considered nonexistent at this point in the calculation. Then the Poisson's equation solver subroutine calculates the resulting potential and electric field components. At this point we of course have $\nabla \times \vec{E} = 0$. Then closing of the switches is simulated by setting the electric field components to zero in the region of the switches. This causes non-zero values of $\nabla \times \vec{E}$ to appear which act as driving terms for eqs. (7) and (11) and initiate the propagating electromagnetic pulse. As mentioned before and as experience has shown, immediately setting the electric field to zero gives rise to undesirable overshoots as the pulse propagates. The overshoot may be reduced although not completely eliminated by setting the field to zero slowly. In practice we do this by setting

$$\vec{E}(T) = \vec{E}_0 \exp(-T/T_0), \tag{44}$$

where $\vec{E}_0$ is the initial electric field and T_0 is a decay time constant. Figure 3 shows the rise of the overshoot as a function of time step for $T_0 = 15\ \Delta T$ as calculated from a one-dimensional analog of eqs. (9 and 11). In the way of contrast, for $T_0 \to 0$ the overshoot approaches 25% after only 120 time steps.

Initial calculations are performed without injection of a particle beam. The progress of the electromagnetic pulse propagation is diagnosed by periodic listings and plotting of all or selected field components. In addition, the open-circuit voltage across the accelerating gap is monitored as well as the electric, magnetic and total energies. The open circuit voltage as a function of time is stored on disk for future processing and for plotting.

After the open-circuit calculations have been performed and the precise timing of the arrival of the accelerating pulse is known, calculations are performed with beam injection. The timing of the beam injection with respect to the accelerating pulse is critical if overshoots and ringing in the accelerated beam energy are unwanted. The beam current is tailored to have a slow exponential rise and fall so that large dI/dT voltages are not generated as the beam passes the gap. After the beam passes the accelerating gap, its energy is calculated at selected

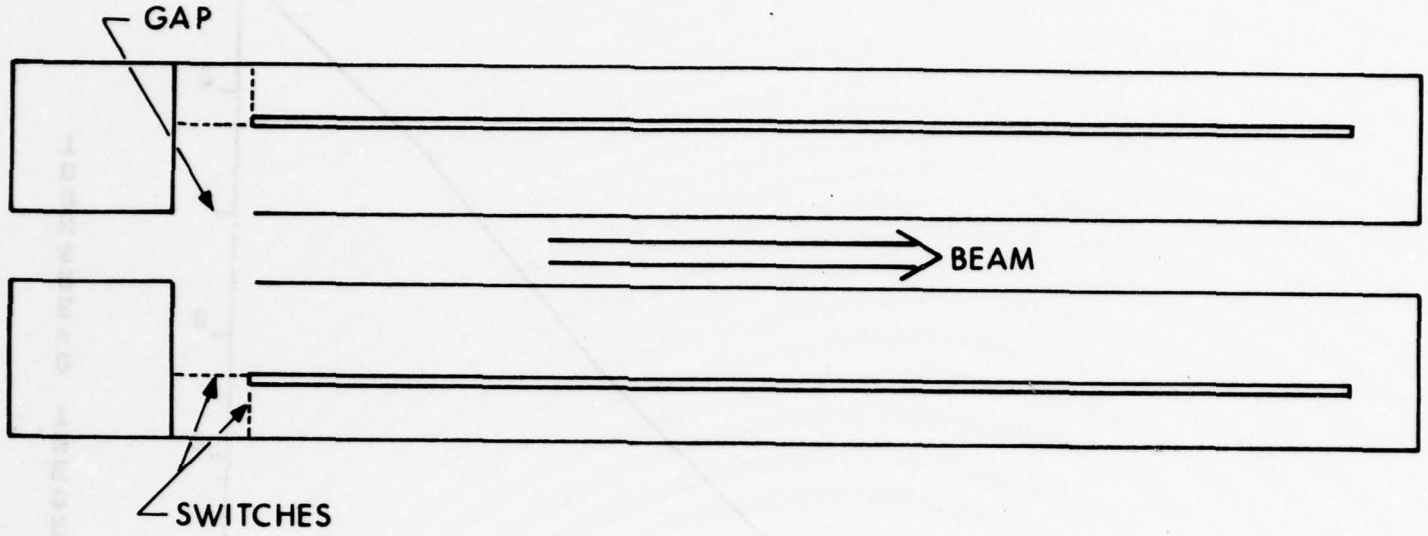

Figure 2. Cavity geometry: the length of the cavity is 1.8 m

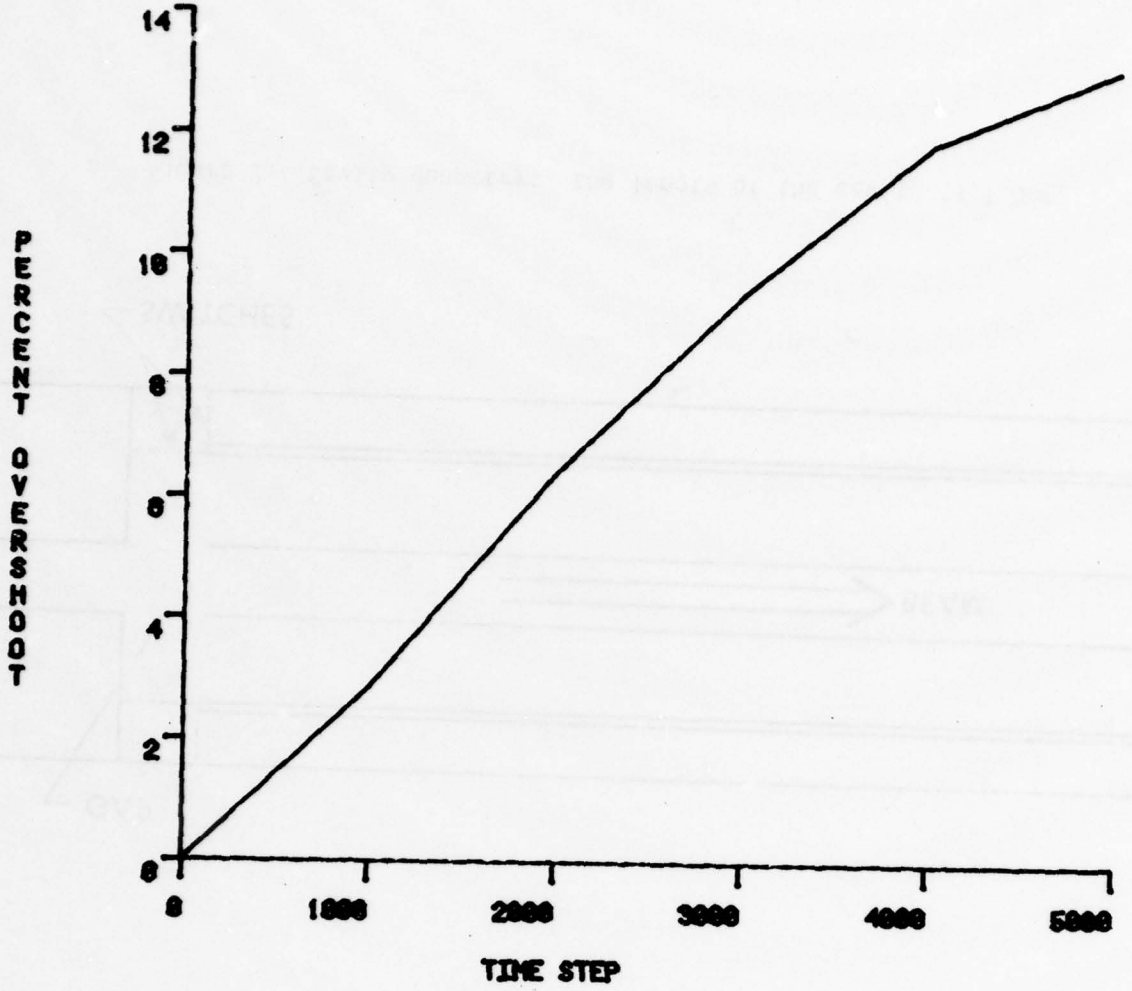

Figure 3. Percent numeric voltage overshoot versus time step for an initial risetime of 15 time steps.

time intervals and radial positions, and this information is stored on disk for subsequent handling. Both solid and hollow beams can be employed.

IV. RESULTS

Figure 2 shows the geometry used for most of the calculations. Some small modifications were however made to test their effect and improve the cavity performance as will be mentioned later. The length of the cavity was chosen to produce an approximately 10 nsec accelerating pulse, and diameters were chosen to provide reasonable proportions and to provide proper impedance ratios. The outer and inner portions of the cavity have characteristic impedances of 20.2 and 61.8 ohms. These are in a ratio of 3.06 to 1 as compared to a 3 to 1 ratio that the transmission[2,3] line analysis concludes is one desirable possibility. Figure 4 shows the open-circuit voltage expected from the principal mode transmission line analysis when the effects of discontinuity at the right end of the cavity and at the gap are neglected. With our simulation code the open circuit voltage shown in Figure 5 is obtained when the initial charge on the middle cylinder is 1000 statvolts ($\sim$ 300 kV). Other parameters of this simulation are $\Delta T = 10^{-11}$ sec, $\Delta R = \Delta Z = 1$ cm, and $T_0 = 1.5 \times 10^{-10}$ sec. Some of the lower amplitude oscillation is due to the previously mentioned numeric dispersion, but the larger amplitude oscillations at 0, 10, 20-22, 30-32, and beyond 40 ns are physical effects due to impedance discontinuities and excitation of higher order modes from the switch closing. Figure 6 shows an intensity field of B_θ 4 ns after the switch closing. A bipolar pulse due to the switch closing is clearly seen in the inner transmission line. Such a pulse is, of course, not included in the idealized transmission line analysis and gives rise to some of the structure in the open circuit voltage.

Of particular interest is how much the risetime of the output voltage pulse is degraded. The most useful single pulse for acceleration is that between about 10 and 20 ns. The polarity change at about 10 ns proceeds from 10% to 90% of the excursion in 0.6 ns. This corresponds to an exponential rise time of 0.27 ns. The excursion around 20 ns takes somewhat longer. To compare with equivalent circuit models of discontinuities it is also of interest to study the risetime degradation of the pulse passing just one discontinuity, for example, the right-hand end of the cavity. Such effects cannot be obtained with the geometry of Fig. 2 since there are two pulses propagating in opposing directions that pass the discontinuity at the same time. Figure 7 illustrates the modification of the geometry employed to overcome this difficulty. The baffles in the inner transmission line provide a tortuous path that slow the pulse traveling through it so that the pulse in the outer transmission line may pass around the discontinuity before the other pulse arrives in the vicinity. An intensity plot of B_θ with this geometry at a

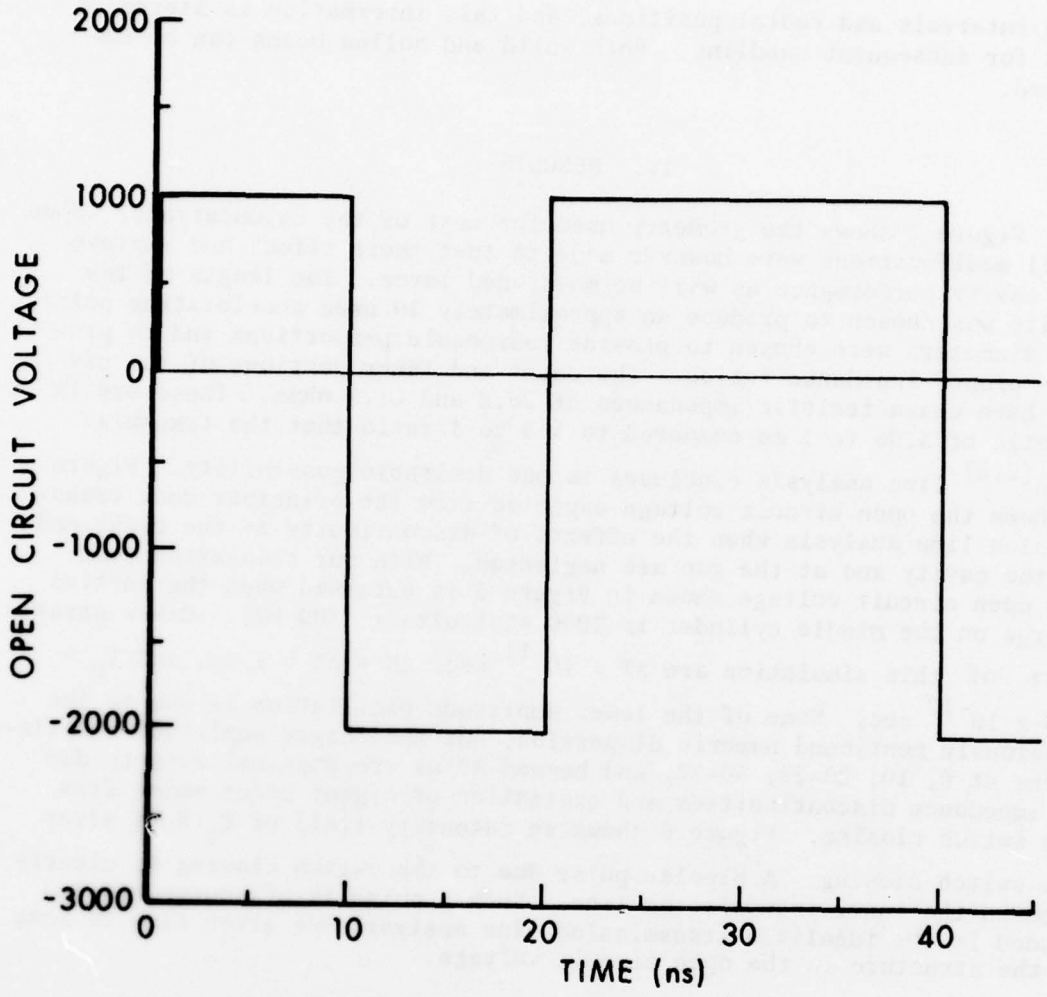

Figure 4. Ideal transmission line open circuit voltage.

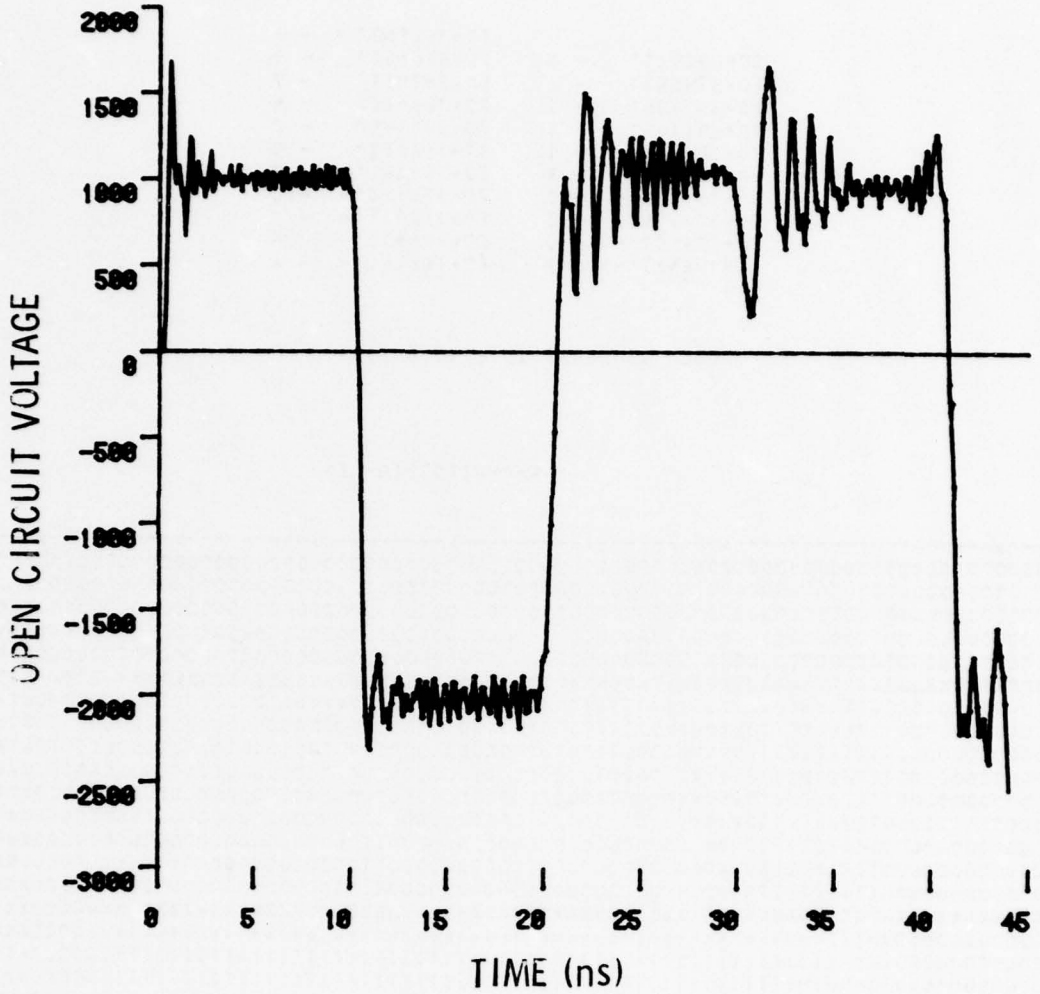

Figure 5. Open circuit voltage - simulation results.

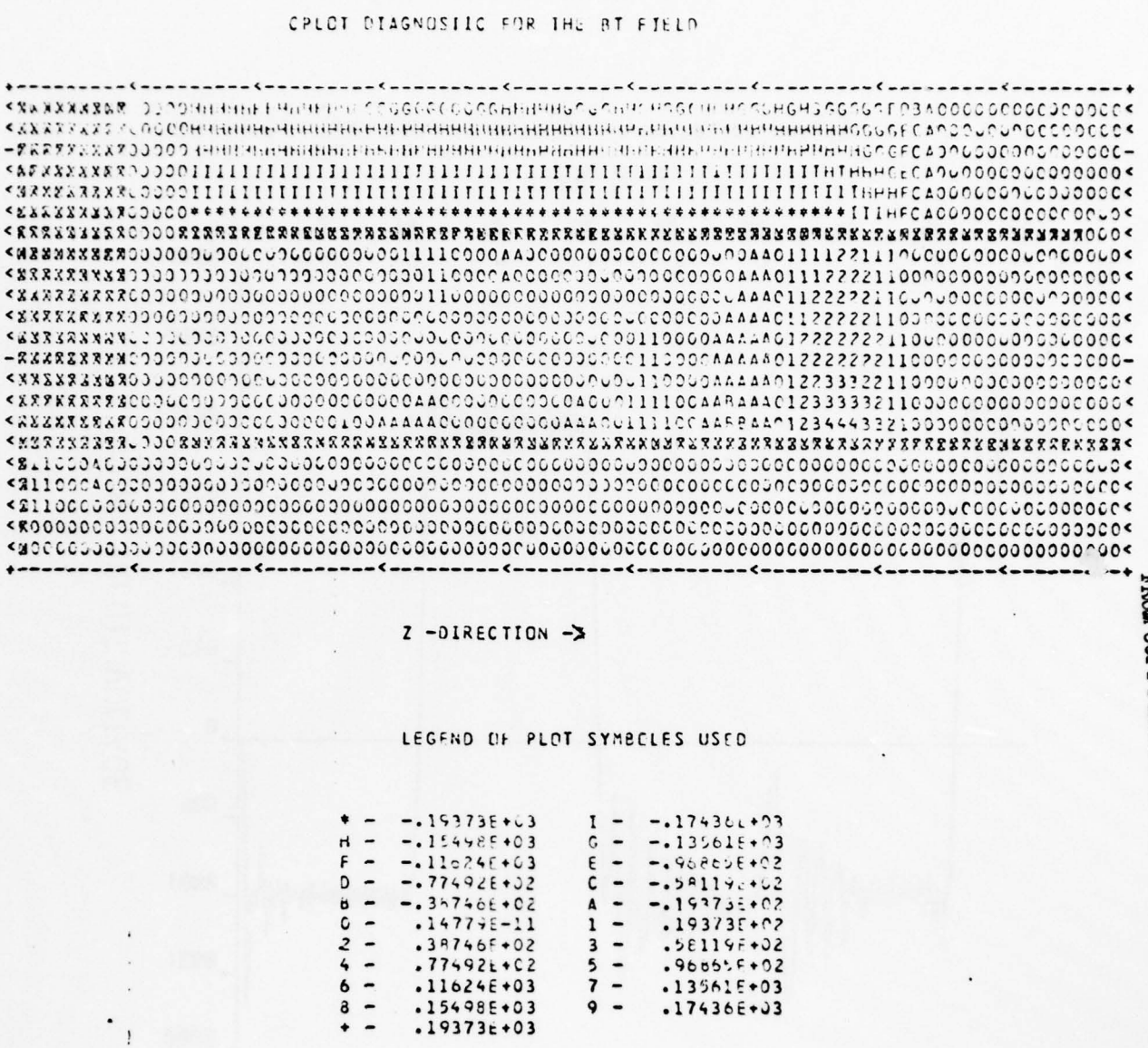

Figure 6. B_θ 4 ns after switch closing. Every other point is plotted in the Z direction.

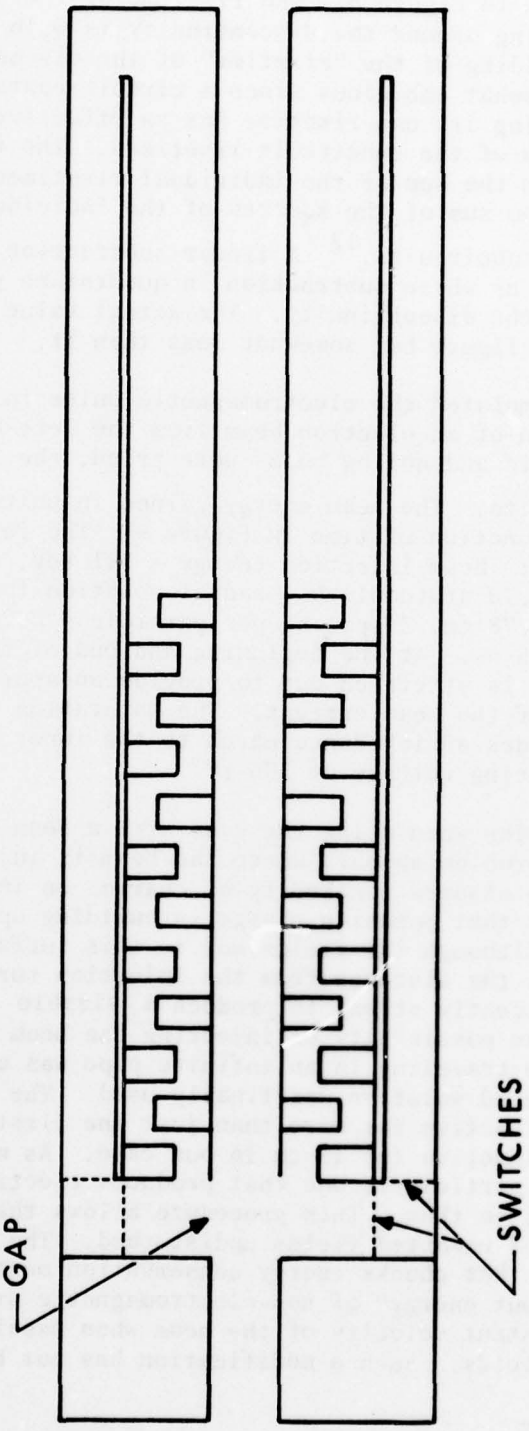

Figure 7. Baffled cavity geometry.

time of 6 ns is shown in Figure 8. The risetime of the simulated voltage pulse just before going around the discontinuity is 0.16 ns and just after it is 0.27 ns. Unfolding of the "risetime" of the discontinuity from these numbers is somewhat ambigious since a circuit containing several subcircuits each having its own risetime has an effective rise that is not a simple function of the subcircuit risetimes. The total circuit risetime is less than the sum of the individual risetimes and approaches the square root of the sum of the squares of the individual risetimes when there are many subcircuits.[12] A linear subtraction of the above risetimes gives 0.11 ns while subtraction in quadrature yields 0.22 ns for the risetime of the discontinuity. The actual value is probably much closer to the second figure but somewhat less than it.

After having simulated the electromagnetic pulse in the cavity, we include the injection of an electron beam from the left-hand side of the inner cylinder. Solid and hollow beams were tried, the latter giving slightly better results. The beam energy gained in units of $m_e c^2$ (511 keV) is shown as a function of time in Figure 9. The following beam parameters were used: beam injection energy = 511 keV, charge per simulation particle = 70.78 statcoulombs, radial position for particle injection = 2.29 and 2.78 cm, Z spacing per particle = 0.25 cm, and beam current risetime 0.15 ns. At the beginning and end of the pulse the Z spacing of particles is stretched out to provide an approximate exponential rise and fall of the beam current. The saturation beam current is 4900 amps that provides an impedance match to the inner transmission line at the accelerating voltage of 300 kV.

Two problems arise when using the code with a beam of charged particles. The first problem appears where the beam is injected. Since the code formulation assumes continuity of charge, an injection of a charged beam implies that opposite charge is building up at the surface of the injection. Although the fields due to this surface charge decay rapidly spatially as the distance from the injection surface increases, the fields are sufficently strong to produce a sizable perturbation of the beam energy. The possibility of injecting the beam "clothed" with fields it would have traveling in an infinite pipe was considered, but a more easily implemented solution was finally used. The solution is to keep the particles inactive for more than just the first half grid spacing; they are kept inactive for 15 cm in our case. As mentioned previously an inactive particle is one that produces electromagnetic fields but does not respond to them. This procedure allows the beam to pass through the region of unwanted fields undisturbed. The only drawback is that the diagnostic that checks energy conservation must be modified to account for the "input energy" of non-electromagnetic origin responsible for maintaining constant velocity of the beam when passing through the injection surface fields. Such a modification has not been implemented yet.

---

[12] *Vacuum Tube Amplifiers*, George E. Valley, Jr., and Henry Wallman, p. 66 and p. 77-78, McGraw-Hill, (1948).

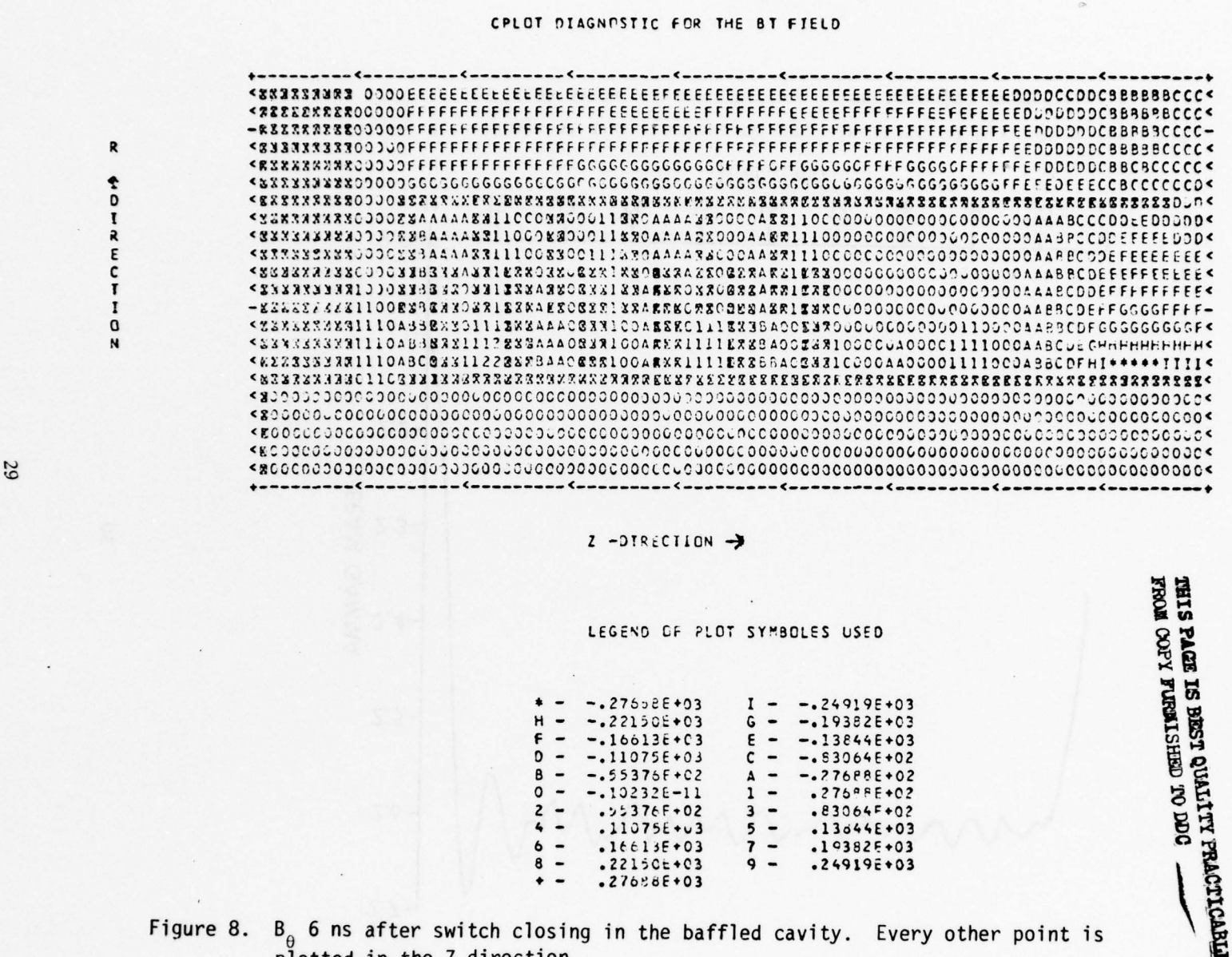

Figure 8. B_θ 6 ns after switch closing in the baffled cavity. Every other point is plotted in the Z direction.

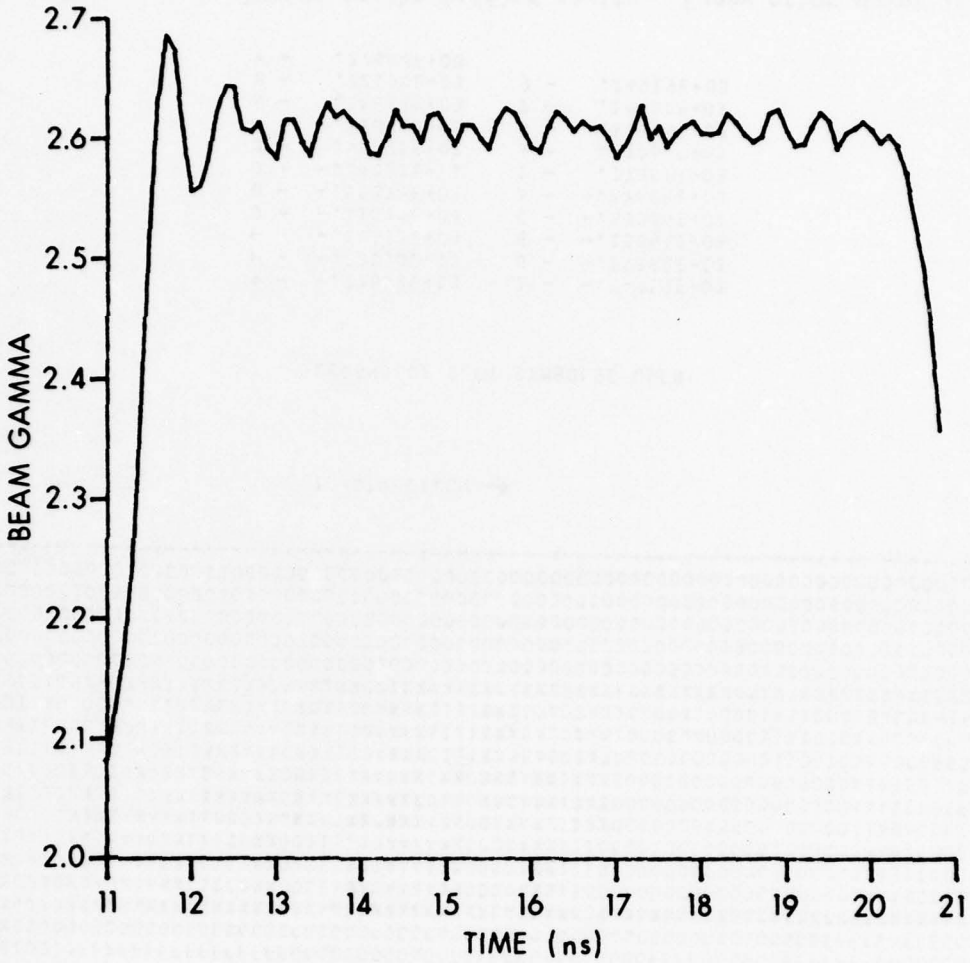

Figure 9. Energy of the accelerated beam in units of $m_c c^2$ as a function of time after switch closing. The injected beam has $\gamma = 2$.

The second problem related to simulation with a beam is numeric: the Cherenkov instability.[13,14] Basically this instability is due to the dispersion properties of the finite difference equations. Since the higher frequencies propagate at less than the speed of light, it is possible for particles traveling at less than the speed of light to travel faster than those higher frequencies. When this happens the particles radiate into these higher order modes via the Cherenkov process. This radiation can reach very high levels and can result in huge perturbations to the particle energies. In our case this radiation rises rapidly from about 60 cm from the beam injection surface. We have been able to live with this problem by diagnosing the accelerated beam energy at 40 cm from the injection surface at which point the Cherenkov instability is of negligible magnitude. Nevertheless this instability is a serious obstacle to the investigation of a beam traveling through several cavities in series. It seems that an entirely different formulation might be required for such a case.

V. DISCUSSION

The above results have shown that the gross features of the simulation code agree rather well with the idealized transmission line analysis for the case of the 3 to 1 impedance ratio investigated. In particular the simulation code shows how well the pulses turn the various corners involved. The simulations have shown that the generation of physical overshoots and higher order mode excitation depends rather sensitively on the detailed geometry of the switch. For example, movement of the lower boundary of the switch one radial position resulted in significantly worse overshoots of the open circuit voltage.

Calculations have been performed for the effects of the discontinuities on the risetimes of the pulses by employing equivalent circuit techniques.[7] Such an analysis leads to a rise that is not a single exponential but is a sum of exponentials. Moreover at the beginning of the pulse, a sharp spike in the reverse direction appears. In our simulations no such reverse spike occurs, although the simulation is consistent with the other features of the equivalent circuit analysis. One is therefore led to the definite conclusion that the reverse spikes are artifacts of the equivalent circuit model and the model does not properly predict very high frequency behavior of the physical system.

The importance of synchronization of the beam pulse with the switch closing was mentioned earlier. If the beam is injected too early the

---

[13] *B.B. Godfrey, "Numerical Cherenkov Instabilities in Electromagnetic Particle Codes," Jour. of Computational Phys., Vol. 15, pp. 504-521 (1974).*

[14] *B.B. Godfrey, "Canonical Momentum and Numerical Instabilities in Particle Codes," Jour. of Computational Phys., Vol. 19, pp. 58-76, (1975).*

dI/dT induced voltage will decelerate the leading portion before the accelerating pulse has arrived at the gap. And if the beam arrives too late, then the leading portion of the beam will see the full open circuit accelerating voltage and receive too much acceleration. A difference of only 0.3 ns in the timing of the beam injection is sufficient to produce significantly poorer results than shown in Figure 9. For many applications a constant accelerated beam energy is required. If magnetic steering is employed in the beam transport system for example, then such a simple consideration as reduction of extraneous radiation dictates the need for a constant energy beam. Thus anything affecting the constant beam output energy is a critical design issue.

At this point it is in order to discuss the various limitations of our computer simulations, their motivation and justifications. The most apparent limitation is the two-dimensional nature of the code. The motivation for this limitation is simple; a 3D code would require excessive computer resources at the present time. Also many interesting geometries can be approximated as 2D structures and be analyzed economically with a 2D code. The geometry analyzed in the present report could in practice be made rotationally symmetric except for the switches; and if several switches were used, they should closely approximate a 2D switch such as that assumed here.

Another limitation is the consideration of only TM modes. Since there is nothing in the geometry to excite transverse electric (TE) modes or to couple TE and TM modes, it would appear wasteful of computer resources to include the TE modes as including them would complicate the programming, nearly double the storage requirements, and more than double the running times of the program. It must be stated, however, that in a working accelerator a stabilizing axial magnetic field would be necessary and would impart helical motion to the particle beam. The leading and trailing ends of a beam with this motion would excite some TE modes. Such excitation is expected to be very weak and not of significance.

Together with all codes using finite difference techniques for solving partial differential equations, the present code requires a finite grid spacing and finite time step and these limit the spatial and temporal resolution of any simulation. Also, due to the resulting dispersion properties of the finite difference equation, the accuracy of the simulation is less than perfect; and for the fine detail errors of 10% can be expected. The finite temporal resolution prevents the simulation of very high frequency instabilities, and other techniques are required to verify that such instabilities can be avoided in a working design. Fortunately analytical procedures exist for investigating some such possible instabilities.

The final limitations of the simulations that we discuss are those related to the particle beam. The main simplification made to the particle motion is to allow only axial motion. Any helical motion is neglected because, as mentioned above, it is expected to be small and not

have significant effects. Not allowing radial motion of the particles is motivated by the desire not to simulate any axial magnetic field at this point. That is to say, if the particles had a radial degree of freedom, an axial magnetic field would be required to prevent radial space charge blow-up of the beam. Additional numeric problems may be introduced under these conditions and it was decided to perform the analysis without these complications at this point and to defer investigation phenomena due to radial particle motion to a later study. Another limitation is that the numeric Cherenkov instability, as discussed earlier, poses a severe restriction to the analysis of high current beams. It has been determined empirically that for low current beams the build-up time for this instability increases considerably, thereby allowing useful simulation of such beams over much longer distances. It is expected that the numeric Cherenkov instability would become worse if radial motion of the beam were permitted.

VI. CONCLUSIONS

Even though the present simulation code has the various limitations just mentioned, the results of the present simulations are interesting and useful. They have shown the sensitivity of the results to the switch geometry, provided quantitative results on the risetimes to be expected from this system, and shown that the beam couples resistively to the accelerating structure. The direction for future work is clear: generalization of the code to remove its limitations. Generalization of the boundaries to allow for boundaries not along the coordinate axis and the allowing of radial motion to the beam should be the first items undertaken, after which new geometries such as radial pulse lines should be investigated. Various approaches to the numeric Cherenkov instability problem should be investigated to determine the most suitable one to apply to our cases. Finally certain interesting geometries are 3D in nature and such problems should be investigated if the necessary resources become available.

ACKNOWLEDGEMENTS

The author is deeply indebted to J. Siambis and A. Drobot of the Naval Research Laboratory for providing their version of the simulation code, advice on using the code, and information and references on the numeric techniques for solving plasma problems. The author would like to thank D. Eccleshall and J.K. Temperley for most useful discussions.

REFERENCES

1. A.I. Pavlovskii, V.S. Bosamykin, G.D. Kuleshev, A.I. Gerasimov, V. A. Tannankin, and A.P. Klementev, Sov. Phys. Dokl. 20, 441 (1975).

2. D. Eccleshall and J.K. Temperley, "Transfer of Energy from Charged Transmission Lines With Applications to Pulsed High-Current Accelerators," Jour. of Appl. Phys., Vol. 49, pp. 3649-3655, July 1978.

3. J.K. Temperley and D. Eccleshall, "Analysis of Transmission-Line Accelerator Concepts," ARBRL Report TR-02067, May 1978. (AD #A056364)

4. J.R. Whinnery and H.W. Jamieson, "Equivalent Circuits for Discontinuities in Transmission Lines," Proc. IRE 32, 98-115, 1944.

5. J.R. Whinnery, H.W. Jamieson, and T.E. Robbins, "Coaxial-Line Discontinuities," Proc. IRE 32, 695-709, 1944.

6. J.R. Whinnery and D.C. Stinson, "Radial Line Discontinuities," Proc. IRE 43, 46-51, 1955.

7. J.K. Temperley, "Analysis of Coupling Region in Transmission-Line Accelerators," ARBRL Report (to be published).

8. Classical Electrodynamics, J.D. Jackson, p. 178, J. Wiley, 1962.

9. J.P. Boris, "Relativistic Plasma Simulation-Optimization of a Hybrid Code," in the Proceedings of the Fourth Conference on Numerical Simulation of Plasmas, Ed. by J.P. Boris and Rama C. Shanny, pp. 3-67, Naval Research Laboratory, 1970.

10. Methods of Theoretical Physics, P.M. Morse and H. Feshbach, p. 116, Mc-Graw Hill, 1953.

11. Space-Charge Flow, Peter T. Kirstein, George S. Kino, and William E. Walters, Chapter 9, McGraw-Hill, 1967. Some typographical errors exist in this chapter. Of interest to us are the following: the factor h^2 should be removed from the denominator before the brackets in eq. (3.1) and the last terms of eqs. (3.2, 3.4) should be multiplied by h^2.

12. Vacuum Tube Amplifiers, George E. Valley, Jr., and Henry Wallman, p. 66 and p. 77-78, McGraw-Hill, (1948).

13. B.B. Godfrey, "Numerical Chrenkov Instabilities in Electromagnetic Particle Codes," Journal of Computational Physics, Vol. 15, pp. 504-521, (1974).

14. B.B. Godfrey, "Canonical Momentum and Numerical Instabilities in Particle Codes," Jour. of Computational Phys., Vol. 19, pp. 58-76, (1975).

APPENDIX

PROGRAM USERS GUIDE

In this appendix we give a description of the overall code logic, the input variables, and the major variables used in the code. In addition the control cards required to run the code on the BRL Cyber 76 will be shown. Although a listing of the Cyber Control Language (CCL) procedure and the in-house coded Poisson solver will be represented, the entire code listing will not be included since the code was not released to us from NRL with the intent of general distribution.

A. Subroutine Structure

Subroutine	Secondary Entry Points	Function
PROP		Main calling routine to allow for variable dimensions with the use of CCL
PROJEC		Actual main routine, handling most of the input, setting up the masks and calling other routines
RELAX		Poisson solver
PROPIN		Initializes electromagnetic field integrator
	PROBEB	Integrates the electromagnetic fields
	DIAGEB	Diagnoses electromagnetic fields by calculating energies and calling listing and plotting routines
	REDSEB	Not used
PUSHIN		Initializes particle pusher
	PUSHP	Integrates particle motion
PPRINT		Field listing
CPLOT		2D field intensity plotter for the line printer
SORCIN		Initializes particle injection
	SOURCE	Injects particles

Subroutine	Secondary Entry Points	Function
DIAGPR		Not used
ZERO		Zeros fields
INJECT		Not used

B. Input Data

All of the input to the program (except some dimension information via CCL) is with NAMELIST read statements. The program contains four namelists: NLMAIN, NLPART, NLMASK, and NLEBPR. The first three are in PROJEC and the last one is in PROPIN. Each namelist is read once except for NLMASK that is read twice, before and after the call to RELAX.

NAMELIST NLMAIN:

Variable	Initialized Value	Function
NF	7	Number of fields plus masks
DR	1	R grid spacing
DZ	1	Z grid spacing
DT	.25	Time steps
C	1	Velocity of light
KØUT	5	Number of major loops - field listings and plottings may be given at the end of each major loop
KINN	1	Number of minor loops - the number of time steps per major loop
KFDI	1	Diagnostic printer control
KFPR	0	Not used
KFRE	0	Not used
KPDI	0	Not used
KPPR	0	Not used
KPRE	0	Not used

Variable	Initialized Value	Function
POT(I)	0	An array that sets the initial electrostatic potential on the conductors. The subscript corresponds to the second subscript of NBOUND (see below in NLMASK)
LPOT	F	If true call RELAX
LPC	F	If true plot initial potential
LPP	F	If true list initial potential
LERC	F	If true plot initial ER field
LERP	F	If true list initial ER field
LEZC	F	If true plot initial EZ field
LEZP	F	If true list initial EZ field
LINT	F	If true integrate field along Z direction to obtain accelerating potential
NIL	1	Innermost radial index for LINT integration
NIH	1	Outermost radial index for LINT integration
NIP	1	Particle energy diagnosed or LINT integration every NIP time steps
	NAMELIST NLPART:	
NPMAX	During procedure call	Don't modify with a read!
NQMAX	During procedure call	Don't modify with a read!
NPS	3	Number of storage locations requried per particle
NZCEL	8	Number of particles injected per Z grid spacing
NRCEL	8	Number of particles injected per R grid spacing

Variable	Initialized Value	Function
MINR	10	Minimum radius of injected particles
MAXR	15	Maximum radius of injected particles
NRPS	0	Number of different particle radii -- redefined after the read
RPOS(I)	0	Radii of the particles - redefined after the read
GAMMA	2	Injected particle γ
SVELO	1	Sign of injection velocity
WPLAS	1	Plasma frequency - redefined if PCHAR $\neq$ 0
PMASS	1	Particle mass
SCHAR	-1	Sign of particle charge
QCHAR		Particle charge - output only
PCHAR	0	Particle charge - if not zero used as particle charge otherwise calculated from WPLAS
PPAR1	0	Rise and fall time of the injected beam in time steps
PPAR2	0	Not used
PPAR3	0	Not used
PPAR4	0	Not used
PPAR5	0	Not used
PPAR6	0	Not used
PPAR7	0	Not used
PPAR8	0	Not used
JSTART	0	Time step to start injecting particles
JSTOP	0	Time step to stop injecting particles

Variable	Initialized Value	Function
LPV	F	If true diagnoses particle energies
IPVD	1	Z position to diagnose particle energies
		NAMELIST NLMASK:
NZMASK	F	If true mask EZ field
NRMASK	F	If true mask ER field
NTMASK		Not used
NAREAS	0	Number of square masks
NBOUND(I,J)	0	Corners of mask in grid units minus 1. Order of I-Z_{min}, Z_{max}, R_{min}, R_{max}
		NAMELIST NLEBPR:
LBNZ	F	If true use periodic boundary conditions
IPRT	6	Unit number for writing energy diagrostics
IPLT	6	Not used
ISAV	6	Unit for storage of energy diagnostics
IFPR		Not used
ISTR	6	Not used
ISTW	6	Not used
NCFR	1	Frequency of plotting in R direction
NCFZ	1	Frequency of plotting in Z direction
NPFR	1	Frequency of listing in R direction
NPFZ	1	Frequency of listing in Z direction
NPWA	1	Not used
LSFR	F	Not used

Variable	Initialized Value	Function
LSPL	F	Not used
LPRT	F	If true print energy diagnostics
LSAV	F	Not used
LPLT	F	If true print out fields
LFPR		If true plot fields
LSTR	F	Not used
LF--	F	If true plot field component --
LP--	F	If true print field component --
NSW	0	Number of slow risetime switches
RTIME	1	Risetime of the switches in time step units
ISW(I,J)	0	Switch boundaries (as in NBOUND)

C. Major Variables Not Appearing as Input

In subroutine PROJEC all of the fields are stored in the array FL(I,J,K) where the first subscript corresponds to the Z position, the second to the R position, and the third to the field type. In the other subroutines the fields are stored under two dimensional arrays (but in the same core locations) EZ, ER, BT, MEZ, MER, JZ and RO; where BT is B_θ, MEZ and MER are the E_Z and E_R masks, RO is ρ, and the other arrays have obvious names. In subroutine RELAX the potential, P, is stored in the core locations used elsewhere for B_θ thus the potential is not available after the electromagnetic propagation calculation begins.

The array CF(I,J) stores the radial differencing coefficients. In RELAX these are the coefficients in eq. (38); and for the propagation, the coefficients are those in eq. (19). The array RPOS contains the radial positions of the particles spaced to provide a uniform current density. Information of the particles is stored in the array PT(I) for the active particles and in the array QT(I) for the inactive particles. In subroutine PUSHIN these arrays are called PSTR and QSTR. Each three consecutive elements of these arrays contain the Z position, R position, and specific momentum (momentum per unit mass) of a particle. As described in the text, the particle momentum is entirely in the Z direction. The variable TIME is an integer variable that counts the number of time steps.

D. Logic Flow

We now give a brief overview of the logic flow of the program. The main routine is PROP with the dimensions for the fields and particle storage assigned from the CCL procedure call. The actual main driver, subroutine PROJEC is called and first initializes the NAMELIST variable. Then the plasma frequencies or particle charges are calculated as well as the RPOS array. The mask for the potential solver are set up and the potential solver is called if requested. Then the propagation masks are set up; and the initializing portions of the particle pushing E & M propagating, and particle subroutines are called. Within the main program loop that is executed next, are calls to the E+M propagation routine, the particle injector, and the particle pusher as well as diagnostics for the accelerating potential, beam energy and field values. Liberal use of comment cards makes the program flow easy to follow.

E. Usage

The program is accessed by attaching an library film containing a CCL procedures and the program object routines. The procedure is called by its name followed by several parameters as follows:

Parameter	1st/2nd Default	Function
NZ	180	Number of mesh line in the Z direction
NR	23	Number of mesh lines in the R direction
NPMAX	45000	Maximum storage for active particles
NQMAX	10000	Maximum storage for inactive particles
LL	5000	Print limit (lines)
COMP	F/T	If specified recompile one or more subroutines
LIST1	L=0/SL,R=3	List the main routine if specified
LIST2	L=0/SL,R=3	List any recompiled routines if specified

If any parameter is left blank in the procedure call, its first default is chosen; if its name is mentioned, the second default is chosen; and if a numeric value or a literal inclosed in $ signs is used, these values are substituted for the parameter in the body of the procedure. When COMP is specified, the procedure itself attaches a file containing an UPDATE library of the source routines and calls UPDATE. Only those routines modified are recompiled; the others are loaded from the object library. When recompiling, the section following the control cards

contains the UPDATE directives followed by the section of data. Otherwise the data section follows the control card section. When the accelerating voltage or the final beam γ are computed and written to TAPE8 or TAPE9 respectively, control cards should be included for the disposition of these files. For example, they may be cataloged, copied to output, and/or handled by calcomp routines. A listing of the driving procedure, subroutine RELAX, and sample inputs follow. The sample input shown is for a special diagnostic run with the baffle geometry shown in Figure 7 and does not initiate beam injection. It is presented merely to show the overall structure of the input.

```
PARTITION VOPROP
.PROC,VOPROP,NZ=180,NR=23,NPMAX=45000,NQMAX=10000,LL=5000,COMP=F/T
LIST1=$L=0$/$SL,R=3$,LIST2=$L=0$/$SL,R=3$,BBBBBB=\DATA.
FTN,I=BBBBBB,OPT,LIST1,SYSEDIT,PL=LL.
IFE,COMP,CHNG.
ATTACH,OLDPL,NRLSOURCE,ID=XRL,PW=*****.
UPDATE.
FTN,I,OPT,LIST2,B=OUT,SYSEDIT.
RETURN,OLDPL,COMPILE.
ENDIF,CHNG.
MAP,PART.
IFE,COMP,C2.
LDSET,PRESET=NGINF.
LOAD,OUT.
LGO.
ELSE,C2.
LDSET,PRESET=NGINF.
LGO.
ENDIF,C2.
.DATA
      PROGRAM PROP (INPUT,OUTPUT,TAPE8,TAPE9,TAPE5=INPUT,
     . TAPE6=OUTPUT,DEBUG=OUTPUT)
      DIMENSION  FL(NZ,NR,7),CF(NR,2)
      DIMENSION PT(NPMAX),QT(NQMAX)
      LEVEL 2,FL
      LEVEL2, PT,QT
      COMMON PT,QT
      COMMON /FLL/ FL
      CALL PROJEC (FL,CF,NZ,NR,PT,QT,NPMAX,NQMAX)
      STOP 777
      END
7
```

```
      SUBROUTINE RELAX (NZ,NR,DZ,DR, POT,ER,EZ,P, MSK,NA,NB,          RELAX     2
     . LPC,LPP,LERC,LERP, LEZC,LEZP                                   RELAX     3
     .     ,RO,CA,CB)                                                 RELAX     4
      DIMENSION EZ(NZ,NR), ER(NZ,NR), P(NZ,NR), MSK(NZ,NR)            RELAX     5
     . ,POT(20), NB(4,20)                                             RELAX     6
     .  ,RO(NZ,NR), CA(NR), CB(NR)                                    RELAX     7
      LEVEL 2, ER,EZ,P,MSK                                            RELAX     8
     .  ,RO                                                           RELAX     9
      LOGICAL LABR(5),LABZ(5),LABI(10),LABC(9),LBC(9),LBT(2)          RELAX    10
      LOGICAL  LPC,LPP, LRB, LERC,LERP, LEZC,LEZP                     RELAX    11
      EQUIVALENCE (LBC(1),LABC(1))                                    RELAX    12
      DATA LBT/"CPLO","PRIN"/                                         RELAX    13
      DATA LABR/" R ]","DIRE","CTIO","N   ","    "/                   RELAX    14
      DATA LABZ/" Z -","DIRE","CTIO","N -%","    "/                   RELAX    15
      DATA LABC/"    ","T DI","AGNO","STIC"," FOR",                   RELAX    16
     .          " THE","    ","FIEL","D  "/                          RELAX    17
      DATA LABI/" ER "," ET "," EZ "," BR "," BT "," BZ ",            RELAX    18
     .          " JR "," JT "," JZ "," RO "/                          RELAX    19
      DATA ITR,LBB /10H;;;;;;;;;;, 2H P/                              RELAX    20
      NP=0                                                            RELAX    21
      DO 10 J=1,NR                                                    RELAX    22
      DO 10 I=1,NZ                                                    RELAX    23
      ER(I,J) = 0.                                                    RELAX    24
      EZ(I,J) = 0.                                                    RELAX    25
   10 P (I,J) = 0.                                                    RELAX    26
      DO 20 N=1,NA                                                    RELAX    27
      NZMIN= NB(1,N) + 1                                              RELAX    28
      NZMAX= NB(2,N) + 1                                              RELAX    29
      NRMIN= NB(3,N) + 1                                              RELAX    30
      NRMAX= NB(4,N) + 1                                              RELAX    31
      IF (NZMIN .LT. 1) NZMIN=1                                       RELAX    32
      IF (NZMAX .GT. NZ) NZMAX=NZ                                     RELAX    33
      IF (NRMIN .LT. 1) NRMIN=1                                       RELAX    34
      IF (NRMAX .GT. NR) NRMAX=NR                                     RELAX    35
      DO 20 J=NRMIN,NRMAX                                             RELAX    36
      DO 20 I=NZMIN,NZMAX                                             RELAX    37
      NP=NP+1                                                         RELAX    38
      P(I,J) = POT(N)                                                 RELAX    39
   20 MSK(I,J) = 0                                                    RELAX    40
      PM = 0.                                                         RELAX    41
      DO 25 I=1,NA                                                    RELAX    42
   25 PM = AMAX1 (PM,ABS (POT(I)))                                    RELAX    43
      IF (PM .EQ. 0.) PM=1.                                           RELAX    44
      PI = 2.* ASIN(1.)                                               RELAX    45
      C1 = 1. /(2./DZ**2 + 2./DR**2)                                  RELAX    46
      CC = C1/DZ**2                                                   RELAX    47
      CD = C1/DR**2                                                   RELAX    48
      CE =-4.*PI*C1                                                   RELAX    49
      C2 = 1./ (2./DZ**2 +4./DR**2)                                   RELAX    50
      CF = C2/DZ**2                                                   RELAX    51
      CG = 4.*C2/DR**2                                                RELAX    52
      CH =-4.*PI*C2                                                   RELAX    53
      DO 28 I=2,NR                                                    RELAX    54
      CA(I) = (I-  .5) *CD/ (I-1)                                     RELAX    55
   28 CB(I) = (I- 1.5) *CD/ (I-1)                                     RELAX    56
C                                                                     RELAX    57
C    MAIN ITERATION SOLUTION OF P                                     RELAX    58
C                                                                     RELAX    59
      OM = 1.7                                                        RELAX    60
      NZM1 =NZ-1                                                      RELAX    61
      NRM1 = NR-1                                                     RELAX    62
      NP = (NR-2) * (NZ-2) - NP                                       RELAX    63
```

```
      DO 30 LOOP=1,400                                                  RELAX      64
      DELV=0.                                                           RELAX      65
      DELAV=0.                                                          RELAX      66
      DO 40 I=2,NZM1                                                    RELAX      67
      DO 40 J=1,NRM1                                                    RELAX      68
      M = AND( MSK(I,J),1)                                              RELAX      69
      IF (M .EQ. 0) GO TO 40                                            RELAX      70
      IF (J .EQ.1) GO TO 50                                             RELAX      71
      DEL = CC* (P(I+1,J) + P(I-1,J)) + CA(J)*P(I,J+1) +CB(J)*P(I,J-1)  RELAX      72
     . +CE*RO(I,J) - P(I,J)                                             RELAX      73
      GO TO 60                                                          RELAX      74
   50 DEL = CF* (P(I+1,1) + P(I-1,1)) + CG*P(I, 2 ) + CH*RO(I,1)        RELAX      75
     .  -P(I,1)                                                         RELAX      76
   60 ADEL = ABS(DEL)                                                   RELAX      77
      DELV = AMAX1 (DELV,ADEL)                                          RELAX      78
      DELAV = DELAV + ADEL                                              RELAX      79
      P(I,J) = P(I,J) + DEL*OM                                          RELAX      80
   40 CONTINUE                                                          RELAX      81
      DELV = DELV/PM                                                    RELAX      82
      DELAV = DELAV/NP/PM                                               RELAX      83
      IF (LOOP .EQ. 1)                 WRITE (6,70) LOOP,DELV,DELAV     RELAX      84
      IF ((LOOP/10) *10 .EQ. LOOP)     WRITE (6,70) LOOP,DELV,DELAV     RELAX      85
   70 FORMAT (" LOOP NO." ,I4, "    LARGEST EPS", 1PE15.4,               RELAX      86
     . "    AVERAGE EPS", E15.4)                                        RELAX      87
      IF ( DELV .LT. 1.E-7) GO TO 80                                    RELAX      88
   30 CONTINUE                                                          RELAX      89
C                                                                       RELAX      90
C    CALCULATE E FIELDS                                                 RELAX      91
C                                                                       RELAX      92
   80 DO 110 J=2,NR                                                     RELAX      93
      ER(1,J) =(P(1,J-1) - P(1,J)) /DR                                  RELAX      94
      DO 110 I=2,NZ                                                     RELAX      95
      ER(I,J) =(P(I,J-1) - P(I,J)) /DR                                  RELAX      96
  110 EZ(I,J) =(P(I-1,J) - P(I,J))/DZ                                   RELAX      97
      DO 120 I=2,NZ                                                     RELAX      98
  120 EZ(I,1) = (P(I-1,1)- P(I,1))/DZ                                   RELAX      99
C                                                                       RELAX     100
C    PAPER PLOTS                                                        RELAX     101
C                                                                       RELAX     102
      NE = NZ/120+1                                                     RELAX     103
      ME = NR/100+1                                                     RELAX     104
      LABC(1)=LBT(1)                                                    RELAX     105
      IF (.NOT. LPC) GO TO 90                                           RELAX     106
      LBC(7) = LBB                                                      RELAX     107
      CALL CPLOT ( P,NZ+1,NZ,NE, NR,1,NR,ME, 0.,0., LABC,LABZ,LABR,     RELAX     108
     . MSK, .F.)                                                        RELAX     109
   90 IF (.NOT. LERC)  GO TO 130                                        RELAX     110
      LBC(7) = LABI(1)                                                  RELAX     111
      CALL CPLOT (ER,NZ+1,NZ,NE, NR,1,NR,ME, 0.,0., LABC,LABZ,LABR,     RELAX     112
     . MSK, .T.)                                                        RELAX     113
  130 IF (.NOT. LEZC) GO TO 140                                         RELAX     114
      LBC(7) = LABI(3)                                                  RELAX     115
      CALL CPLOT (EZ,NZ+1,NZ,NE, NR,1,NR,ME, 0.,0., LABC,LABZ,LABR,     RELAX     116
     . MSK, .T.)                                                        RELAX     117
  140 CONTINUE                                                          RELAX     118
      LABC(1)=LBT(2)                                                    RELAX     119
      IF (.NOT. LPP) GO TO 100                                          RELAX     120
      LBC(7) = LBB                                                      RELAX     121
      CALL PPRINT ( P,NZ,1,NZ,1, NR,1,NR,1, 0,LABC)                     RELAX     122
  100 IF(.NOT. LERP) GO TO 150                                          RELAX     123
      LBC(7) = LABI(1)                                                  RELAX     124
      CALL PPRINT (ER,NZ,1,NZ,1, NR,1,NR,1, 0,LABC)                     RELAX     125
  150 IF(.NOT. LEZP) GO TO 160                                          RELAX     126
```


45

```
      LHC(7) = LABI(3)                                                  RELAX    127
      CALL PPRINT (EZ,NZ,1,NZ,1, NR,1,NR,1, 0,LABC)                     RELAX    128
C                                                                       RELAX    129
C     RESET MASK                                                        RELAX    130
C                                                                       RELAX    131
  160 DO 170 J=1,NR                                                     RELAX    132
      DO 170 I=1,NZ                                                     RELAX    133
  170 MSR(I,J) = ITR                                                    RELAX    134
      RETURN                                                            RELAX    135
      END                                                               RELAX    136
```

```
$IN,STMFZ,T100.
ACCOUNT,******, SHNIDMAN, B390   X5889
ATTACH,ML,NRL OBJECT,ID=ARL,PW=********.
LIBRARY,ML.
VOPROP,,,10,10,10000,COMP.
?
*ID SMART
*I PPRINT.40
      DO 80 I=1,MM
      R = I-1.5
      DO 80 J=1,NN
   80 A(J,I) = A(J,I)*R
?
 $NLMAIN
 KPDI=1,
 DT=1.E-11,
 C=3.E10,
 KINN=600,KOUT=1,
 LPOT=T,
 POT=1000.,  0.,0.,0.,0.,0.,  1000.,0.,1000.,0.,1000.,0.,1000.,0.,1000.,0.,
  1000.,0.,
 $
 $NLPART
 NZCEL=4.,
 NRCEL=2,
 PCHAR=-70.7784,
 PMASS=1.342296E-16,
 PPAR1=15.,
 MAXR=3,
 MINR=2,
 JSTART=10000,
 $
 $NLMASK
 NZMASK=T,
 NRMASK=T,
 NAREAS=18,NBOUND(1,1) = 26,171,14,15,  26,179,4,5,  178,179,0,22,  0,1,0,5,
 0,18,4,22,  18,179,21,22,
 26,30,8,14,  33,37,5,11,  40,44,8,14,  47,51,5,11,  54,58,8,14,  61,65,5,11,
 68,72,8,14,  75,79,5,11,  82,86,8,14,  89,93,5,11,  96,100,8,14,  103,107,5,11,
 $
 $NLMASK
 $
 $NLEBPR
 LPRT=T,
 LPER=T,
 LPLT=T,
 NCFZ=2,
 NSW=1,  ISW=18,27,14,21,
 RTIME=15.,
 $
?
```

DISTRIBUTION LIST

No. of Copies	Organization
12	Commander Defense Documentation Center ATTN: DDC-DDA Cameron Station Alexandria, VA 22314
1	Commander US Army Materiel Development and Readiness Command ATTN: DRCDMD-ST, N. Klein 5001 Eisenhower Avenue Alexandria, VA 22333
1	Commander US Army Aviation Research and Development Command ATTN: DRSAV-E 12th and Spruce Streets St. Louis, MO 63166
1	Director US Army Mobility Research and Development Laboratory Ames Research Center Moffett Field, CA 94035
2	Commander US Army Electronics Research and Development Command Technical Support Activity ATTN: DELSD-L DRSEL-TL-BG/Dr.Schneider Fort Monmouth, NJ 07703
1	Commander US Army Communications Rsch and Development Command ATTN: DRDCO-PPA-SA Fort Monmouth, NJ 07703
4	Commander US Army Harry Diamond Labs ATTN: DELHD-RBC, Dr. A. Kehs Dr. Bromborsky Dr. R. Puttkamp DELHD-PP, Dr. Sokoloski 2800 Powder Mill Road Adelphi, MD 20783
1	Commander US Army Missile Research and Development Command ATTN: DRDMI-R Redstone Arsenal, AL 35809
1	Commander US Army Missile Materiel Readiness Command ATTN: DRSMI-AOM Redstone Arsenal, AL 35809
1	Commander US Army Tank Automotive Research & Development Cmd ATTN: DRDTA-UL Warren, MI 48090
3	Commander US Army Armament Research and Development Command ATTN: DRDAR-TSS (2 cys) DRDAR-TD, Dr. Weigle Dover, NJ 07801
1	Commander US Army Armament Materiel Readiness Command ATTN: DRSAR-LEP-L, Tech Lib Rock Island, IL 61299
1	Commander US Army Foreign Science and Technology Center ATTN: Dr. Thomas Caldwell 220 Seventh Street, NE Charlottesville, VA 22901
1	Director US Army TRADOC Systems Analysis Activity ATTN: ATAA-SL, Tech Lib White Sands Missile Range NM 88002
1	HQDA (DAMA-ARZ-A, MAJ Acklin) Washington, DC 20310

48

DISTRIBUTION LIST

No. of Copies	Organization
1	HQDA (DAMA-CSM-CS, LTC Townsend) Washington, DC 20310
1	Commander US Army Research Office ATTN: Dr. Herman Robl P. O. Box 12211 Research Triangle Park NC 27709
2	Director US Army BMD Advanced Technology Center ATTN: ATC-D, Dr. L.J. Havard Dr. T. Roberts P. O. Box 1500 Huntsville, AL 35807
1	US Army Research and Standardization Gp (Europe) ATTN: Dr. Alfred K. Nedoluha Box 65 FPO New York 09510
1	Commander Naval Surface Weapons Center ATTN: WR-401, C.M. Huddleston Silver Spring, MD 20910
2	Commander Naval Research Laboratory ATTN: Code 77002 Dr. M. Friedman Dr. J. Siambis Washington, DC 20375
1	National Bureau of Standards ATTN: Dr. J. Leiss Director, Center for Radiation Research Room 229, Bldg. 245 Washington, DC 20234
1	Director ATTN: J. C. Nall P. O. Box 1925 Washington, DC 20505
2	Director Lawrence Livermore Laboratory ATTN: L-306, Dr. R.J. Briggs L-306, Dr. T. Fessenden University of California P. O. Box 808 Livermore, CA 94550
2	Director Sandia Laboratories ATTN: Dr. B. Miller, Fusion Rsch Department Dr. K. Prestwich, Pulsed Power Applications & Operations Division Albuquerque, NM 87115
1	Austin Research Associates, Inc. ATTN: Dr. L. Sloan 600 West 28th Street Austin, TX 78705
1	Battelle Columbus Laboratories ATTN: Dr. C. T. Walters Associate Manager, Physical Sciences Section 505 King Avenue Columbus, OH 43201
1	JAYCOR ATTN: Dr. M. Dowe 205 South Whiting Street Suite 500 Alexandria, VA 22304
1	Maxwell Laboratories, Inc. ATTN: Dr. Trivelpiece 9244 Balboa Avenue San Diego, CA 92123

DISTRIBUTION LIST

No. of Copies	Organization
2	Physical Dynamics, Inc. ATTN: Dr. K. Brueckner Mr. John Shea P. O. Box 556 La Jolla, CA 92038
1	Physics International Company ATTN: Dr. Sid Putnam 2700 Merced Street San Leandro, CA 94577
1	Rand Corporation ATTN: Dr. S. Kassel 2100 M Street, NW Washington, DC 20002
2	Science Applications, Inc. ATTN: Dr. M. P. Fricke Dr. R. Shanny 1200 Prospect Street La Jolla, CA 92037
1	Science Applications, Inc. ATTN: Dr. R. Johnston 2680 Hanover Street Palo Alto, CA 94304
1	Ian Smith, Inc. ATTN: Dr. I. Smith 3115 Gibbons Drive Alameda, CA 94501
1	University of California Lawrence Berkeley Laboratory ATTN: Dr. Dennis Keefe Berkeley, CA 94720
1	University of California School of Engineering and Applied Science ATTN: Prof. C. T. Leondes, Engineering Systems Dept. Los Angeles, CA 90027

Aberdeen Proving Ground

Dir, USAMSAA
ATTN: DRXSY, Dr. J. Sperrazza
DRXSY-MP, H. Cohen
Cdr, USATECOM
ATTN: DRSTE-SG-H